The types of [*PIN*$^+$] prions and liquid-like aggregates formed by the yeast protein Rnq1 are controlled by interactions between its non-prion and prion domains

Irina L. Derkatch[1,2,*], Michele L. Kadnar[1], Susan W. Liebman[2], Monica Andrade[1], Anna P. Fomitchova[1], Dania M. Maldonado[2]

1. Department of Microbiology, NYU School of Medicine, New York, NY, USA
2. Department of Pharmacology, University of Nevada Reno, Reno, NV, USA
* Corresponding Author: iderkatch@unr.edu

Current addresses:
Monica Andrade: Department of Biological and Vision Sciences, College of Optometry, State University of New York, New York, NY 10036
Anna P. Fomitchova: New York Medical College / New York Metropolitan Hospital, New York, NY

Abstract:

Prions are self-propagating protein conformations usually existing as amyloid aggregates. [*PIN*$^+$], a prion form of the Rnq1 protein frequently found in wild and laboratory yeast strains, facilitates both the *de novo* formation and destabilization of other yeast prions, and affects aggregation and toxicity of human misfolding disease proteins expressed in yeast. Rnq1 consists of a short N-terminal domain with no confirmed function (the non-prion domain, NPD) and a C-terminal QN-rich domain sufficient for [*PIN*$^+$] formation and maintenance (prion domain, PD). The prion domain carries four discrete QN-rich regions. None of these are essential for stable [*PIN*$^+$] prion maintenance, and any two are sufficient. In the current work, a genetic screen identified the T27P mutation in the beginning of the NPD that blocks transmission of the [*PIN*$^+$] prion state from wild type Rnq1 (Rnq1$_{WT}$) to mutant Rnq1$_{T27P}$. However, the mutation does not prevent overexpressed Rnq1$_{T27P}$ from taking on a prion conformation *in vivo* or the assembly of Rnq1$_{T27P}$ amyloid fibers *in vitro*. Furthermore like [*PIN*$^+_{WT}$], the newly formed [*PIN*$^+_{T27P}$] promotes the *de novo* appearance of the Sup35-based prion [*PSI*$^+$]. This indicates that the mutation specifically creates a barrier for the transmission of the prion state from [*PIN*$^+_{WT}$] to Rnq1$_{T27P}$. Because fluorescence microscopy shows that Rnq1$_{T27P}$ efficiently joins [*PIN*$^+_{WT}$] aggregates, the barrier is likely due to the inability of Rnq1$_{T27P}$ to propagate the [*PIN*$^+_{WT}$] conformation once Rnq1$_{WT}$ is gone. Indeed, the analysis of [*PIN*$^+_{T27P}$] cultures resulting from rare transmission events from [*PIN*$^+_{WT}$] confirmed that initially the [*PIN*$^+_{T27P}$] prions are very unstable and are lost from most mitotic progeny. However, studies of [*PIN*$^+_{T27P}$] lineages for >100 generations revealed that such prions gradually stabilize. While some [*PIN*$^+_{T27P}$] lineages reach stability indistinguishable from that of [*PIN*$^+_{WT}$], others reach different levels of stability that do not change upon further propagation, indicative of the formation of distinct [*PIN*$^+_{T27P}$] prion conformations. This supports the idea that the underlying reason for the transmission barrier is that Rnq1$_{T27P}$ is unable to efficiently propagate the specific [*PIN*$^+_{WT}$] prion strain conformation but can undergo conformational adaptation even in non-selective conditions. Such conformational adaptation was previously observed when a prion was transmitted from [*PIN*$^+_{WT}$] to Rnq1 fragments lacking one or more QN-rich regions in the PD. Indeed, we now find that deletion of the first QN-rich region of the PD considerably reduces the transmission barrier created by the T27P mutation, indicating that the NPD can create conformational constraints on a particular region of the PD. Another finding supporting the idea of the effect of the NPD on aggregation properties of the PD is that Rnq1$_{T27P}$ readily forms non-amyloid liquid-like droplets which Rnq1$_{WT}$ does not form. Based on comparison of the Rnq1 homologs from other species, the T27P mutation is located in one of two conserved regions of the NPD, the other region being the interaction site for the Sis1 chaperone involved in [*PIN*$^+$] maintenance and toxicity upon Rnq1 overexpression. The current findings, together with prior data, suggest that the entire Rnq1 protein contributes to its aggregation and prionization properties, and that these properties are essential for Rnq1 function, possibly in controlling the aggregation of other proteins.

Keywords: yeast, prion, prion variant, prion strain, amyloid, liquid-like droplets, transmission barrier, Rnq1, [*PIN*$^+$], [*RNQ*$^+$], Sup35, [*PSI*$^+$].

Abbreviations: NPD – non-prion domain, PD – prion domain, WT – wild type, GuHCl-guanidine hydrochloride, 5-FOA - 5-fluoroorotic acid,

Introduction

The prion hypothesis postulates that some proteins can acquire stable unconventional conformations and pass these conformations to newly synthesized molecules with the same primary sequence. Amyloid, the β-sheet-rich fibers with protein molecules stacked on one another, is the structural basis for most prions and prion-like self-propagating protein conformations (Chuang et al., 2018; Dobson, 2017; Ke et al., 2020). Prions and amyloids attracted attention due to their association with so called protein misfolding diseases that are associated with and, probably, caused by the formation of amyloid aggregates. The list of such diseases is expanding quickly from bona fide prion diseases, such as scrapie in sheep, mad cow disease in cattle and Creutzfeldt-Jakob disease in humans (Joshi and Ahuja, 2023), that prompted the development of the paradigm of protein-based inheritance (Ayers et al., 2020, to much more common neurodegenerative diseases, such as Alzheimer's and Parkinson's, as well as type 2 diabetes and, possibly cancer.

Many protein misfolding diseases can be both sporadic, usually with a later age of onset, and hereditary, due to mutation in amyloid-forming proteins. This underscores the importance of uncovering the cellular mechanisms that drive and inhibit protein misfolding, as well as conformational changes within specific aggregation-prone proteins that lead to disease related aggregation. Prion diseases can also be infectious. Luckily, protective measures were stepped up in recent decades to prevent iatrogenic human to human transmission. Animal to human transmission is usually prevented by transmission barriers when differences in primary sequences in protein homologs from different species make interspecies transmission of the prion state inefficient. However, as we learned from the appearance of novel human disease resulting from a cross of the transmission barrier between humans and cows, variant Creutzfeldt-Jakob disease, such barriers are not absolute. An important aspect of the problem is possible rapid adaptation of prion conformations in a new host after rare across-the barrier transmission events.

Prion research has been greatly facilitated by the discovery of naturally occurring prions in the yeast *Saccharomyces cerevisiae* (Wickner, 1994). The same underlying amyloid structure of yeast prions and mammalian disease aggregation-prone proteins and evolutionary conservation of genes makes yeast an excellent model for studying protein aggregation and mechanisms that control it. Many yeast prions carry long terminally located QN-rich domains that are unfolded in soluble proteins but are critical and frequently sufficient for taking on prion conformations and maintainng them. Hence their name – prion domains. Similar QN-rich domains also drive aggregation of some human disease proteins. [*PSI*$^{+}$], the prion form of a

translation termination factor Sup35 is the most extensively studied yeast prion, and many important findings come from the [*PSI*$^+$] prion research. One such finding is prion-prion interaction. Initially it was postulated that overexpression of a prion-forming protein should induce the *de novo* appearance of its respective prion conformation (Wickner, 1994), and initial data for [*PSI*$^+$] appeared to support this idea (Derkatch et al., 1996). However, once [*PSI*$^+$]s were eliminated by the addition to yeast culture media of low concentrations of guanidine hydrochloride that appears to be a generic prion curing agent efficient induction of [*PSI*$^+$] by Sup35 overexpression was no longer possible. This is because the [*PIN*$^+$] prion required for induction of [*PSI*$^+$] was cured (Derkatch et al., 1997.)

[*PIN*$^+$] is formed by the Rnq1 protein (Sondheimer and Lindquist, 2000; Derkatch et al., 2001.) Rnq1 consists of a short N-terminal domain with no confirmed function (the non-prion domain, NPD) and a C-terminal QN-rich domain sufficient for [*PIN*$^+$] formation and maintenance (prion domain, PD). The prion domain carries four discrete QN-rich regions. None of these are essential for stable [*PIN*$^+$] prion maintenance, and any two are sufficient (Kadnar et al., 2010.)

Finally, it is known that most prion forming proteins, both mammalian and yeast can form multiple prion strains manifesting different conformations of these proteins in prion aggregates (Bessen and Marsh, 1992; Bessen et al., 1995; Derkatch et al., 1996; Bradley et al., 2002).

Results and Discussion

Genetic screen for Rnq1 mutations.

The goal of the screen was to identify the Rnq1 mutant alleles that, when substituted for wild type protein in a [*PIN*$^+$] strain (Pin$^+$ phenotype), will lead to a Pin$^-$ phenotype. Here, the Pin phenotype is determined as facilitation (Pin$^+$) or lack of facilitation (Pin$^-$) of the *de novo* appearance of the [*PSI*$^+$] prion upon overexpression of the [*PSI*$^+$] prion forming protein, Sup35, or its prion domain, Sup35NM.

The screen is schematically shown in Figure 1A. First, *CEN LEU2* plasmids carrying PCR-mutagenized *RNQ1* driven by its native non-mutagenized promoter and followed by its native non-mutagenized terminator sequence were transformed into the [*PIN*$^+$][*psi*$^-$] strain where the chromosomal copy of *RNQ1* was deleted and [*PIN*$^+$] was maintained by a similar but *URA3*-marked Rnq1$_{WT}$ plasmid. Transformants were patch onto synthetic media selective for all plasmids and passaged on this media twice by replica plating allowing for ~30 generations of co-expression of Rnq$_{WT}$ and Rnq1$_{mutant}$. Second, the maintainer plasmid was selectively shuffled out on media with 5-FOA selective for other plasmids. Third, [*PSI*$^+$] was induced in SGal-UraHis

media. Fourth, cells carrying [*PSI*$^+$] were selected on synthetic media lacking adenine not selective for plasmids. Selection on adenineless media is based on nonsense suppression of the *ade1*-14 (UGA) mutation due to the recruitment of the Sup35 protein, a translation termination factor, into [*PSI*$^+$] prion aggregates. For Pin$^+$ cultures, thick, even if heterogenic, growth was observed over the entire patch. For the presumptive Pin$^-$ cultures either no growth or rare Ade$^+$ colonies were observed on media lacking adenine.

The Pin$^-$ phenotype of the candidate mutants was confirmed by re-transformation experiments where mutant plasmids were isolated and individually tested according to the same scheme. Also, the Pin$^-$ phenotype was confirmed by fluorescence microscopy of cells grown on the [*PSI*$^+$] inducing SGal-LeuHis media using the YFP tag as a reporter for Sup35 aggregation in the [*PSI*$^+$] cells (in the [*psi*$^-$] cells fluorescence is evenly distributed; Patino and Lindquist, 1996; Zhou et al., 2001). Finally, the Pin$^-$ phenotype was confirmed by colony purifying yeast from SGal-LeuHis onto YPD, where [*psi*$^-$] and [*PSI*$^+$] cells form, respectively red and white colonies.

Out of ~15,000 yeast transformants screened, 24 were either firmly Pin$^-$, or their Pin phenotype was dramatically reduced. 23 of these carried plasmids with nonsense mutations in the N-terminal part of *RNQ1*, either within its NPD, or before the middle of the second QN-rich domain within the PD (Figure 1B). This is consistent with the requirement of the PD of RNQ1 for the maintenance of the [*PIN*$^+$] prion (Vitrenko et al., 2007; Kadnar et al., 2010). Noteworthy, the coverage of near-cognate codons by nonsense mutations suggested that the screen was saturating even though usually only one mutation was detected on each plasmid sequenced (data not shown). The fact that no nonsense or missense mutations were detected beyond the middle of the second QN-rich domain can be explained based on our earlier deletion analysis of Rnq1 (Kadnar et al., 2010). Because the PD of Rnq1 is redundant and none of the QN-rich domains is essential for the maintenance of the [*PIN*$^+$] prion and the Pin$^+$ phenotype, a mutation inactivating just one of the four QN-rich regions would not affect [*PIN*$^+$] propagation.

The only mutant that passed the screen and did not belong to the above mentioned group carried the T27P mutation in the beginning of the N-terminal NPD of Rnq1 (Figure 1C). After Rnq1$_{WT}$ was shuffled out, the cultures expressing Rnq1$_{T27P}$ were almost Pin$^-$ but were not exacty Pin$^-$. Compared to the control experiment where Rnq1$_{WT}$ was substituted with the empty vector (EV), there were occasional Ade$^+$ [*PSI*$^+$] colonies on adenineless media (Figure 1B). Fluorescence analysis revealed that in rare Rnq1$_{T27P}$ cells with [*PSI*$^+$] aggregates these aggregates were similar to the [*PSI*$^+$] aggregates in the control cultures where Rnq1$_{WT}$ was substituted with Rnq1$_{WT}$. Also, in the YPD test, rare [*PSI*$^+$] colonies induced in the Rnq1$_{T27P}$ cultures manifested the same array of [*PSI*$^+$] strains as in the cultures from the Rnq1$_{WT}$ to

$Rnq1_{WT}$ transmissions. Thus, the cultures expressing $Rnq1_{T27P}$ had a dramatically reduced but typical Pin^+ phenotype

$Rnq1_{T27P}$ can form [*PIN*$^+$] *de novo* upon overexpression and these [*PIN*$^+$] are not deficient in [*PSI*$^+$] induction.

The genetic screen described above was based on the Pin^+ phenotype of *de novo* induction of the [*PSI*$^+$] prion. Thus, the following hypotheses explaining to the dramatic reduction of the Pin^+ phenotype were considered. (1) The [*PIN*$^+$] prion state is not transmitted from $Rnq1_{WT}$ to $Rnq1_{T27P}$ during the co-expression step (transmission barrier). (2) $Rnq1_{T27P}$ is deficient in acquiring / maintaining the [*PIN*$^+$] prion conformation. (3) Most cells in the $Rnq1_{T27P}$ cultures carry the prion after $Rnq1_{WT}$ has been shuffled out, but this [PIN^+_{T27P}] prion is unable to induce [*PSI*$^+$], e.g. due to a defect in the heterologous prion-prion cross-seeding (Derkatch et al., 2001).

In general, the *de novo* appearance of prions can be induced by their transient overexpression, and the process of prion aggregate formation can be monitored by microscopy by attaching a fluorescent tag to a prion forming protein (Zhou et al., 2001). However, $Rnq1_{WT}$ does not form *de novo* [*PIN*$^+$] aggregates upon overexpression when attached to a C-terminal GFP family tag (Derkatch et al., 2001), so this obvious experiment was skipped.

Instead, we performed an experiment that would test both the second and third hypotheses together. During the first step, the *de novo* induction of [PIN^+_{T27P}] was attempted by overexpression of the untagged $Rnq1_{T27P}$ driven by the inducible *CUP* promoter. During the second step, [*PSI*$^+$] induction was attempted as described above. For this experiment, the *CEN URA3* plasmid carrying the *CUP-RNQ1*$_{T27P}$ construct and the *CEN LEU2* plasmid carrying *RNQ1* under its original promoter were introduced into a [*pin*$^-$][*psi*$^-$] *rnq1-Δ* strain already encompassing the *GAL-SUP35NM-YFP* [*PSI*$^+$] inducing construct. Expression of *CUP-RNQ1*$_{T27P}$ was induced on the synthetic $CuSO_4$ containing media selective for all plasmids. Then, yeast were replica plated to media without $CuSO_4$, where $Rnq1_{T27P}$ is not overexpressed and [PIN^+_{T27P}] is not induced *de novo* but can be maintained, and to the [*PSI*$^+$] inducing SGal plasmid selective media. Finally, yeast were transferred to the adenineless [*PSI*$^+$] selective media. Indeed, [*PSI*$^+$] was equally efficiently induced in the $Rnq1_{T27P}$ and control $Rnq1_{WT}$ samples (data not shown). Several other versions of this experiment were performed where [PIN^+_{T27P}] and [*PSI*$^+$] were induced simultaneously or with more or less cell generations between the induction steps. No difference was observed compared to control experiments with $Rnq1_{WT}$ suggesting that the T27P mutation does not affect the *de novo* [*PIN*$^+$] prion formation, its maintenance or facilitation of [*PSI*$^+$] formation by these [*PIN*$^+$]s.

$Rnq1_{T27P}$ forms typical amyloid fibers *in vitro*.

Another way to assess aggregation properties of $Rnq1_{T27P}$ was to test the ability of the purified protein to form amyloid fibers *in vitro*. Bacterially expressed $Rnq1_{T27P}$ and $Rnq1_{WT}$ were tested for the propensity to form amyloid *in vitro*. Incubation of proteins encompassing Thioflavin T (ThT) resulted in a shift of the ThT excitation spectrum and increase of ThT fluorescence at 483 nm, indicative of amyloid formation. Sigmoidal fluorescence kinetics was consistent with the presence of a rate-limiting nucleation step followed by a fiber growth phase. Lag phase was similar for the $Rnq1_{T27P}$ and $Rnq1_{WT}$ samples (data not shown).

Transmission electron microscopy (TEM) revealed >1 μm-long $Rnq1_{T27P}$ fibers. As in the $Rnq1_{WT}$ samples, fibers were ~ 20nm wide, not branched and consisted of laterally associated thinner fibers. The only possible difference in the fiber appearance was that $Rnq1_{T27P}$ fibers were slightly more twisted.

The T27P mutation creates a barrier for the transmission of the prion state from [PIN^{+}_{WT}] to $Rnq1_{T27P}$.

The next hypothesis tested was if the T27P affects the transmission of the prion conformation from $Rnq1_{WT}$ to $Rnq1_{T27P}$. If the transmission block were absolute, all cells in the post-shuffle $Rnq1_{T27P}$ would be expected to be [*pin*$^{-}$]. The incomplete Pin^{-} phenotype observed in our experiments would be more consistent with prion absence in most but not all post-shuffle $Rnq1_{T27P}$ cells. To test this possibility, the *CEN LEU2* $Rnq1_{T27P}$ or control $Rnq1_{WT}$ and empty vector plasmids were introduced into the same strain as used in the genetic screen ([*PIN*$^{+}$][*psi*$^{-}$] *rnq1Δ* carrying the *CEN URA3* $Rnq1_{WT}$ maintainer and *CEN HIS3 GAL-SUP35NM-YFP*). The scheme of the experiment is presented in Figure 3A. After the maintainer was shuffled out after ~30 generations of plasmid co-existence and cultures were transferred to SD-LeuHis, yeast were colony purified on SD-LeuHis, individual colonies were patched on SD-LeuHis and analyzed for the Pin phenotype.

Indeed, we found that 2-3% of the cells in the $Rnq1_{T27P}$ post-shuffle cultures retained Pin^{+} phenotype, whereas the remaining 97-98% were clearly Pin^{-} (see sample plate on Figure 3B). For example, in one experiment 7 out of 286 $Rnq1_{T27P}$ colonies were Pin^{+}. $Rnq1_{T27P}$ to $Rnq1_{T27P}$ transmission was 100% efficient (398/398), and $Rnq1_{T27P}$ to empty vector transmission did not yield Pin^{+} isolates (0/156). The Pin^{+} phenotype of the exceptional $Rnq1_{T27P}$ cultures varied in strength, from indistinguishable from $Rnq1_{WT}$ to $Rnq1_{WT}$ transmissions to moderately reduced, which could be seen as heterogenic growth on adenineless media, but it always was stronger

than in transmissions without colony purification (compare Figure 3B and 1C). This finding supports the idea of the transmission barrier between $Rnq1_{WT}$ and $Rnq1_{T27P}$.

To estimate the strength of the transmission barrier between $Rnq1_{WT}$ and $Rnq1_{T27p}$ two factors should be considered. First, in our experiments, we allowed for ~30 generations of $Rnq1_{T27P}$ expression in the presence of [*PIN*$^+$] maintained by $Rnq1_{WT}$. We performed a control experiment where, in a similar experimental system, Rnq1 fragment lacking the first QN-rich region ($Rnq_{\Delta B1}$), which has a very mild transmission barrier with $Rnq1_{WT}$ (Kadnar et al., 2010) was introduced into the [*PIN*$^+$] strain simultaneously with the disruption of the chromosomally encoded *RNQ1*$_{wt}$ with the *HIS3* gene. In this experiment, all 12 obtained disruptant His$^+$ colonies were Pin$^+$, confirming that one generation of co-expression is sufficient for the transmission (Kadnar and Derkatch, unpublished). Thus, the 0.02 transmission rate after 30 generations may correspond to 0.0007 transmission rate per generation. However, the interesting question is the transmission rate per generation per propagon. This cannot be answered convincingly because the exact number of [*PIN*$^+$] propagons in unknown.

Conformational adaptation of [*PIN*$^+_{T27P}$] prions after crossing the transmission barrier. The existence of the transmission barrier from the [*PIN*$^+$] prion formed by $Rnq1_{WT}$, [*PIN*$^+_{WT}$], to $Rnq1_{T27P}$, i.e. that $Rnq1_{T27P}$ is unable to attain and/or stably maintain the specific prion conformation in which $Rnq1_{WT}$ is present in [*PIN*$^+_{WT}$] is supported by the finding that $Rnq1_{T27P}$ can efficiently take on a prion conformation and form the [*PIN*$^+_{T27P}$] prion *de novo*. However, it was still not clear, what causes the dramatic reduction of Pin$^+$ in cells expressing $Rnq1_{T27P}$ after shuffle: a very low transmission rate, or high instability of [*PIN*$^+_{T27P}$] prions resulting from such transmissions.

To address this issue, we analyzed the stability of the [*PIN*$^+_{T27P}$] prions in the progeny of cells that acquired them by transmission. For this experiment, the [*PIN*$^+_{T27P}$] prion containing yeast cultures were colony purified from the Pin$^+$ patches obtained from individual colonies after transmission (see e.g. two Pin$^+$ patches on Figure 3B). However, while the Pin status of the cultures was determined on adenineless media after [*PSI*$^+$] induction, these colony purifications were done from SD-LeuHis where yeast were transferred right after plasmid shuffle. This was done to avoid selection for [*PIN*$^+_{T27P}$] carrying cells. Individual colonies obtained on SD-LeuHis were patched onto SD-LeuHis and subjected to another round of the Pin phenotype analysis. Colonies were analyzed for all Pin$^+$ isolates obtained after the initial transmission, regardless of the strength of their Pin$^+$ phenotype. Noteworthy, in this experiment, cells were propagated for

the same number of generations as after the plasmid shuffle in the first round of colony purifications described above.

We found that, while most cells in the Pin$^+$ cultures we analyzed were [*pin*-], indicative of [*PIN*$^+_{T27P}$] instability, the proportion of prion-containing cells increased to ~15%.

This analysis was repeated for a total of 7 rounds the same way. The key findings are: (1) the stability of [*PIN*$^+_{T27P}$] gradually increased in rounds 3 and 4, cultures with more stable [*PIN*$^+_{T27P}$] could be predicted from the strength of the Pin$^+$ phenotype in the previous round; (2) a stable [*PIN*$^+_{T27P}$] derivative was isolated in round 3 (87/88); (3) by round 5 lineages with still unstable [*PIN*$^+_{T27P}$] started falling into two distinct groups – those where stability of [*PIN*$^+_{T27P}$] reached 50% or more and those, where it remained at ~25%; at this point no further stabilization was observed.

Data for the abovementioned experiments is not shown (will be included in the revised version), but see results for similar experiments for the Rnq1$_{WT}$ to Rnq1$_{T27P}$ controls in Figure 4.

In essence, these data suggest that the T27P mutation puts conformational constraints onto Rnq1$_{T27P}$. It cannot form a stable [*PIN*$^+$] prion strain conformationally identical to the one formed by Rnq1$_{WT.}$ And, apparently, Rnq1$_{T27P}$ forms a different [*PIN*$^+_{T27P}$] strain(s) when it forms them *de novo*. However, within [*PIN*$^+_{T27P}$] there is a possibility of gradual conformational adaptation towards prion conformations that are more stable. Interestingly, such conformational adaptation appears to be a multistep process, but not all of the prion conformations that undergo conformational adaptation can reach 100% stability. Some are obviously “stuck” as metastable prion variants. Recently, similar ideas were discussed by King (2022) for [*PSI*$^+$] prion strains that he obtained with Sup35 constructs carrying different mutations, albeit in the PD.

The transmission barrier created by the T27P mutation located in NPD is considerably reduced by the deletion of the first QN-rich region within Rnq1 PD.

Transmission barriers with subsequent conformational adaptation were previously uncovered for the transfer of prion conformations between [*PIN*$^+_{WT}$] and Rnq1 fragments lacking one or more QN-rich regions in the PD (see Figure 1B for a schematic presentation of the structural organization of the Rnq1 PD). We analyzed the transfer of prion conformations between (1) [*PIN*$^+_{WT}$] and Rnq1 prion fragments carrying the T27P mutation (e.g. ∆B1C2$_{T27P}$), and (2) between stable [*PIN*$^+$] prions in cells expressing only such Rnq1 fragments e.g. ∆B1C2 and either full length Rnq1$_{T27P}$ or a corresponding deletion variant carrying the mutation, e.g. ∆B1C2$_{T27P}$ (Figure 4 all panels and data not shown). Overall, the results indicate that the

transmission barrier created by the T27P mutation located in NPD is considerably reduced by the deletion of the first QN-rich region within Rnq1 PD.

Unlike Rnq1$_{WT}$, Rnq1$_{T27P}$ readily forms liquid-like droplets when expressed in [*pin*$^-$] cells. As mentioned above, Rnq1$_{WT}$, when fused to bulky C-terminal fluorescent tags from the GFP family, does not form visible aggregates and does not form [*PIN*$^+$[*de novo* when overexpressed in [*pin*$^-$] strains (Derkatch et al., 2001). One possible explanation for this is that the last QN-rich region of the PD of Rnq1 is involved in prion formation. This idea is supported by our earlier observation that transmission of the prion state from Rnq1$_{WT}$ to Rnq1 fragments lacking this domain is inefficient even though it can form prions alone when overexpressed (Kadnar et al., 2010). However, when a similar construct, Rnq1$_{T27P}$-YFP is overexpressed in in [*pin*$^-$] yeast, it readily forms line and dot aggregates similar to those seen [*PIN*$^+_{WT}$] cells upon the introduction of the Rnq1-YFP construct. Furthermore, dot-like aggregates are formed by Rnq1$_{T27P}$-YFP in [*pin*$^-$] cells at close to physiological levels of expression. However, these aggregates are dissolved upon a short-term Hexanediol (Hex) treatment, suggesting that they are not amyloid but liquid-like droplets (Figure 5). This further supports the idea that the NPD mutation T27P modulates aggregation and conformational properties of QN-rich regions within the PD of Rnq1.

Materials and Methods

Strains and Plasmids

Derivatives of the original [*PIN*$^+$][*psi*$^-$] isolate of the yeast 74-D694 yeast strain (1Y1; Derkatch et al., 1997) were used in all experiments, unless specifically mentioned. The genotype of 74-D694 is *MAT***a** *ade1-14* (UGA) *leu2-3,112 his3-Δ200 trp1-289*(UAG) *ura3-52*. The [*PIN*$^+$][*psi*$^-$] *rnq1-Δ* 74-D694 strain used for the genetic screen, YID146.2, was constructed as described in Kadnar et al. (2010). In this strain the entire *RNQ1* ORF is seamlessly disrupted and [*PIN*$^+$] is maintained by the *CEN URA3* plasmid carrying Rnq1$_{WT}$ ORF driven by the native *RNQ1* promoter and followed by the native *RNQ1* terminator sequence (Rnq1$_{WT}$). Unless specifically mentioned, the strain also carries the *CEN HIS3 GAL-SUP35NM-YFP* plasmid allowing to monitor the presence of [*PIN*$^+$] through the de novo [*PSI*$^+$] induction.

An isogenic [*pin*$^-$][*psi*$^-$] isolate of 74-D694 (1G4; Derkatch et al., 1997) obtained by curing the [*PIN*$^+$] prion on media containing 5mM guanidine hydrochloride (GuHCl; Tuite et al., 1981)

was used as a control. An isogenic [*pin*$^-$][*psi*$^-$] isolate of YID146 was obtained by transient removal of the $Rnq1_{WT}$ plasmid (Kadnar et al., 2010).

The pRS416-based (Sikorski and Hieter, 1989) *CEN URA3* plasmid carrying $Rnq1_{WT}$ ORF driven by the native *RNQ1* promoter and followed by the native *RNQ1* terminator sequence ($Rnq1_{WT}$), is described in Kadnar et al. (2010). The $Rnq1_{T27P}$ plasmid (as well as other plasmids in the genetic screen) are pRS415-based, i.e. *LEU2 CEN*, but otherwise are identical to $Rnq1_{WT}$.

The pRS413-based *CEN HIS3 GAL-SUP35NM-YFP* plasmid (Kadnar et al., 2010) carries *SUP35NM-YFP* encoding the prion domain of the [*PSI*$^+$]-forming Sup35 protein fused to the YFP reporter (from Derkatch and Liebman, 2007) placed under control of the inducible *GAL1* promoter. In the pRS416-based *CEN URA3 CUP-RNQ-CFP* (Kadnar et al., 2010), a fusion of complete wild type *RNQ1* ORF to *CFP* is driven by the *CUP1* promoter.

Bacterial expression constructs for $Rnq1_{WT}$ and $Rnq1_{T27P}$ are pJC45-based and express N-terminally 10xHIS tagged proteins (Kadnar et al., 2010).

Yeast Media and cultivation

Standard yeast media and cultivation procedures were used (Rose et al., 1990; Sherman et al., 1987). Unless specifically mentioned yeast were gown at 30^{0}C on solid synthetic glucose containing media selective for plasmid maintenance (e.g. SD-UraLeuHis). The *GAL* promoter was induced on synthetic media selective for plasmid maintenance supplemented with 2% galactose as a single carbon source (e.g. SGal-LeuHis). The CUP promoter was induced by supplementing SD media with $CuSO_4$; unless specifically mentioned CuSO4 was added to the final concentration of 20μM. To selectively eliminate plasmids with the *URA3* marker (Boeke et al., 1884), yeast were passaged twice on solid media supplemented with 5-fluoroorotic acid (5-FOA) selective for other plasmids.

Recombinant protein purification

Recombinant protein purification was essentially as described in Kadnar et al. (2010). Specifically, *Escherichia coli* BL21-AI One Shot cells (Invitrogen) were transformed with the pJC45-based $Rnq1_{WT}$ and $Rnq1_{T27P}$ expression constructs. Transformants were grown in LB medium supplemented with 100 μg/ml ampicillin at 37^{0}C until the mid-log phase (OD_{600}=0.4) when protein expression was induced by 1mM IPTG and 0.2% L-arabinose for 1.5 h. Cells were harvested by centrifugation (4^{0}C, 1600 x g) and lysed by gentle agitation in lysis buffer (100mM NaH2PO4 pH 7.4, 350mM NaCl, 8M urea) for 1h at room temperature. Cell debris was removed by centrifugation at 20,000 x g for 10 min. Supernatant was incubated for 2 h with Ni-NTA

Sepharose (Qiagen) equilibrated with the lysis buffer. Then the slurries were transferred to columns and washed extensively with the lysis buffer. Rnq1 was eluted with the lysis buffer containing 250mM imidazole. UV absorption at 280nm was used to identify protein containing fractions. Centricons (Millipore) were used for concentrating proteins. Protein concentration was determined by the BCA assay (Pierce). Purity of recombinant proteins was estimated by SDS-PAGE as >95%.

Analysis of *in vitro* fiber formation

Analysis of *in vitro* fiber formation was performed essentially as in Kadnar et al. (2010). Specifically, 200 μl reactions were assembled in the fiber formation buffer (1M urea, final concentration; 100mM NaH_2PO_4 pH 7.4; 300mM NaCl) in the presence of 5 μM thioflavin T (ThT). Fiber formation was monitored by ThT fluorescence (LeVine, 1999) in a Molecular Devices SpectraMax M-5 plate reader (λ_{ex}=450 nm; λ_{em}=483 nm; 24^0C). Readings were taken every 15 min, samples were shaken for 5 sec prior to each reading. Experiments were performed in duplicate and repeated at least 3 times.

Transmission Electron Microscopy (TEM)

TEM was performed at the Image Core Facility and the NYU School of Medicine. Following the incubation to allow for amyloid fiber formation in the assembly buffer, protein / fiber suspensions were diluted 2.5-fold in water and 4 μl were applied onto the carboncoated 400 mesh Cu/Rh grids (Ted Pella Inc.). The grids were washed 3 times with water to get rid of urea present in the assembly buffer, and negatively stained with 1% uranyl acetate (twice briefly and then for 5 min at 25^0C). Images were obtained using Philips CM12 TEM supplied with a Gatan 1k61k digital camera and processed using the Gatan Digital Micrograph software.

Fluorescence Microscopy

For most experiments, cells were observed using an Axioplan2 Zeiss microscope. Images of representative fields were captured with a Zeiss Axiocam digital camera and processed with Improvision OpenLab software.

References

Ayers JI, Paras NA, Prusiner SB. Expanding spectrum of prion diseases. Emerg Top Life Sci. 2020 Sep 8;4(2):155-167. doi: 10.1042/ETLS20200037. PMID: 32803268.

Bessen RA, Marsh RF. Identification of two biologically distinct strains of transmissible mink encephalopathy in hamsters. J Gen Virol. 1992 Feb;73 (Pt 2):329-34. doi: 10.1099/0022-1317-73-2-329. PMID: 1531675.

Bessen RA, Kocisko DA, Raymond GJ, Nandan S, Lansbury PT, Caughey B. Non-genetic propagation of strain-specific properties of scrapie prion protein. Nature. 1995 Jun 22;375(6533):698-700. doi: 10.1038/375698a0. PMID: 7791905.

Boeke JD, LaCroute F, Fink GR. A positive selection for mutants lacking orotidine-5'-phosphate decarboxylase activity in yeast: 5-fluoro-orotic acid resistance. Mol Gen Genet. 1984;197(2):345-6. doi: 10.1007/BF00330984. PMID: 6394957.

Bradley ME, Edskes HK, Hong JY, Wickner RB, Liebman SW. Interactions among prions and prion "strains" in yeast. Proc Natl Acad Sci U S A. 2002 Dec 10;99 Suppl 4(Suppl 4):16392-9. doi: 10.1073/pnas.152330699. Epub 2002 Jul 30. PMID: 12149514; PMCID: PMC139899.

Chuang E, Hori AM, Hesketh CD, Shorter J. Amyloid assembly and disassembly. J Cell Sci. 2018 Apr 13;131(8):jcs189928. doi: 10.1242/jcs.189928. PMID: 29654159; PMCID: PMC5963839.

Derkatch IL, Chernoff YO, Kushnirov VV, Inge-Vechtomov SG, Liebman SW. Genesis and variability of [PSI] prion factors in Saccharomyces cerevisiae. Genetics. 1996 Dec;144(4):1375-86. doi: 10.1093/genetics/144.4.1375. PMID: 8978027; PMCID: PMC1207691.

Derkatch IL, Bradley ME, Zhou P, Chernoff YO, Liebman SW. Genetic and environmental factors affecting the de novo appearance of the [PSI+] prion in Saccharomyces cerevisiae. Genetics. 1997 Oct;147(2):507-19. doi: 10.1093/genetics/147.2.507. PMID: 9335589; PMCID: PMC1208174.

Derkatch IL, Liebman SW. Prion-prion interactions. Prion. 2007 Jul-Sep;1(3):161-9. doi: 10.4161/pri.1.3.4837. Epub 2007 Jul 6. PMID: 19164893; PMCID: PMC2634589.

Dobson CM. The Amyloid Phenomenon and Its Links with Human Disease. Cold Spring Harb Perspect Biol. 2017 Jun 1;9(6):a023648. doi: 10.1101/cshperspect.a023648. PMID: 28062560; PMCID: PMC5453392.

Joshi T, Ahuja N. The Prion Basis of Progressive Neurodegenerative Disorders. Interdiscip Perspect Infect Dis. 2023 Feb 14;2023:6687264. doi: 10.1155/2023/6687264. PMID: 36825209; PMCID: PMC9943612.

Kadnar ML, Articov G, Derkatch IL. Distinct type of transmission barrier revealed by study of multiple prion determinants of Rnq1. PLoS Genet. 2010 Jan 22;6(1):e1000824. doi: 10.1371/journal.pgen.1000824. PMID: 20107602; PMCID: PMC2809767.

Ke PC , Zhou R , Serpell LC , Riek R , Knowles TPJ , Lashuel HA , Gazit E , Hamley IW , Davis TP , Fändrich M , Otzen DE , Chapman MR , Dobson CM , Eisenberg DS , Mezzenga R . Half a century of amyloids: past, present and future. Chem Soc Rev. 2020 Aug 7;49(15):5473-5509. doi: 10.1039/c9cs00199a. Epub 2020 Jul 7. PMID: 32632432; PMCID: PMC7445747.

King CY. The Mutability of Yeast Prions. Viruses. 2022 Oct 25;14(11):2337. doi: 10.3390/v14112337. PMID: 36366434; PMCID: PMC9696419.

LeVine H 3rd. Quantification of beta-sheet amyloid fibril structures with thioflavin T. Methods Enzymol. 1999;309:274-84. doi: 10.1016/s0076-6879(99)09020-5. PMID: 10507030.

Patino MM, Liu JJ, Glover JR, Lindquist S. Support for the prion hypothesis for inheritance of a phenotypic trait in yeast. Science. 1996 Aug 2;273(5275):622-6. doi: 10.1126/science.273.5275.622. PMID: 8662547.

Rose M, Winston F, Hieter P. (1990) Methods in yeast genetics — A laboratory course manual by pp 198. Cold Spring Harbor Laboratory Press, Cold Spring Harbor, New York. ISBN 0-87969-354-1

Sikorski RS, Hieter P. A system of shuttle vectors and yeast host strains designed for efficient manipulation of DNA in Saccharomyces cerevisiae. Genetics. 1989 May;122(1):19-27. doi: 10.1093/genetics/122.1.19. PMID: 2659436; PMCID: PMC1203683.

Sherman, F., Fink, G., Hicks, J. (1987) *Methods in Yeast Genetics: A Laboratory Course Manual.* Cold Spring Harbor Laboratory Press. ISBN 9780879691974

Tuite MF, Mundy CR, Cox BS. Agents that cause a high frequency of genetic change from [psi+] to [psi-] in Saccharomyces cerevisiae. Genetics. 1981 Aug;98(4):691-711. doi: 10.1093/genetics/98.4.691. PMID: 7037537; PMCID: PMC1214469.

Vitrenko YA, Pavon ME, Stone SI, Liebman SW. Propagation of the [PIN+] prion by fragments of Rnq1 fused to GFP. Curr Genet. 2007 May;51(5):309-19. doi: 10.1007/s00294-007-0127-0. Epub 2007 Apr 6. PMID: 17415568; PMCID: PMC2597802.

Wickner RB. [URE3] as an altered URE2 protein: evidence for a prion analog in Saccharomyces cerevisiae. Science. 1994 Apr 22;264(5158):566-9. doi: 10.1126/science.7909170. PMID: 7909170.

Zhou P, Derkatch IL, Liebman SW. The relationship between visible intracellular aggregates that appear after overexpression of Sup35 and the yeast prion-like elements [PSI(+)] and [PIN(+)]. Mol Microbiol. 2001 Jan;39(1):37-46. doi: 10.1046/j.1365-2958.2001.02224.x. PMID: 11123686.

Figure 1

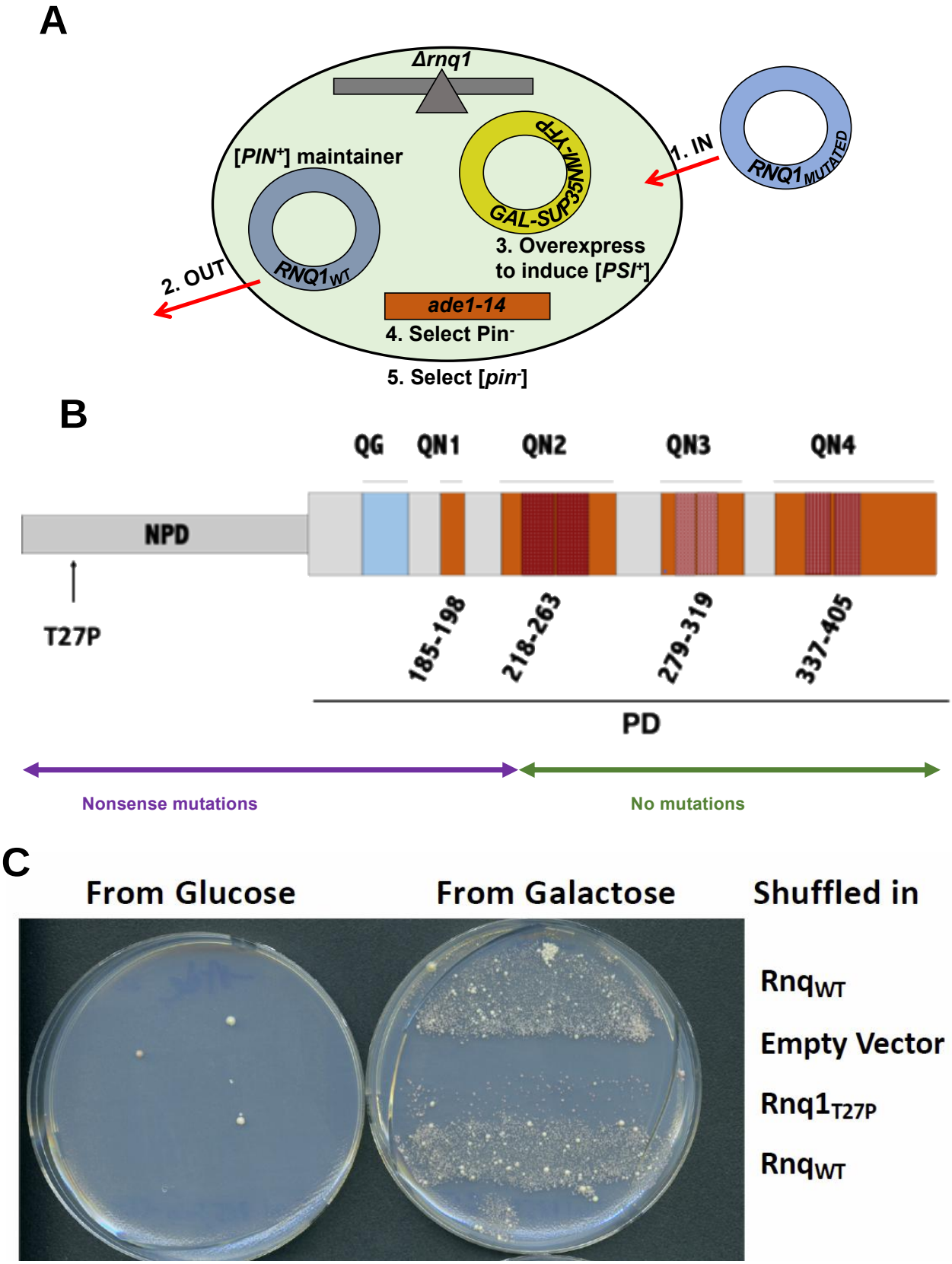
A
Δrnq1
[PIN+] maintainer
RNQ1WT
GAL-SUP35NM-YFP
1. IN
RNQ1MUTATED
2. OUT
3. Overexpress
to induce [PSI+]
ade1-14
4. Select Pin-
5. Select [pin-]
B
QG
QN1
QN2
QN3
QN4
NPD
T27P
185-198
218-263
279-319
337-405
PD
Nonsense mutations
No mutations
C
From Glucose
From Galactose
Shuffled in
RnqWT
Empty Vector
Rnq1T27P
RnqWT

Figure 1. Genetic screen for mutation in Rnq1 that, when substituted for Rnq1$_{WT}$ in a [*PIN*$^+$] strain (Pin$^+$ phenotype), will lead to a Pin$^-$ phenotype. (**A**) Scheme of the genetic screen (see text). (**B**) Structural organization of the Rnq1 protein. Shown are NPD with the position of the T27P mutation and PD with four distinct QN-regions (see text; adapted from Kadnar et al., 2010). (**C)** The T27P mutation, Rnq1$_{T27P}$, leads to a dramatic reduction of the Pin$^+$ phenotype when substituted for Rnq1$_{WT}$ in a [*PIN*$^+$] strain. Shown is growth on SD-Ade media at 30^{0}C for 14 days after substituting Rnq1$_{T27P}$ for Rnq1$_{WT}$ (as described for the genetic screen) and growing yeast either on the [*PSI*$^+$] inducing SGal-LeuHis media (two passages), or on the control SD-LeuHis. Each row includes patches of 5 independent transformants.

Figure 2

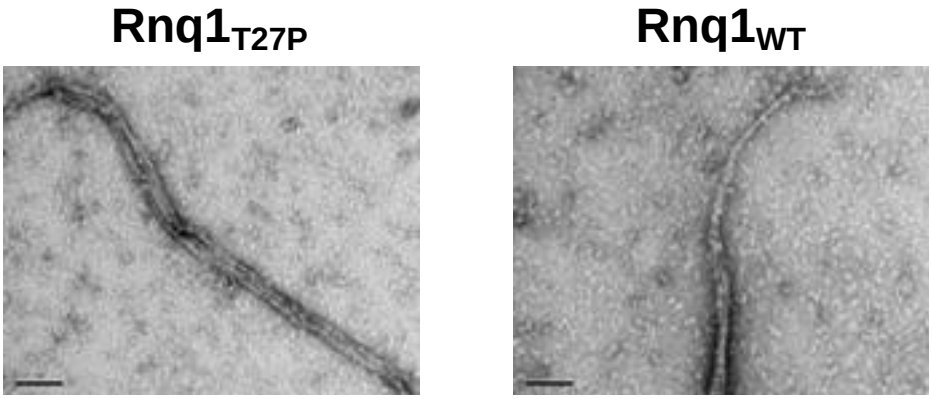

Figure 2. Transmission electron micrographs of negatively stained $Rnq1_{T27P}$ and $Rnq1_{WT}$ fibers. Scale bar corresponds to 50 nm

Figure 3

A

[*PIN*$^+$][*psi*$^-$] *rnq1*Δ strain carrying Rnq1$_{WT}$ and *GAL-SUP35NM-YFP*

↓

Transformation With Rnq1$_{T27P}$ or controls (EV, Rnq1$_{WT}$)

↓

Plasmid shuffle

↓

Colony purification

↓

Patches from colonies

↓

[*PSI*$^+$] induction

↓

[*PSI*$^+$] selection

B

Rnq1$_{WT}$ **Rnq1$_{T27P}$**

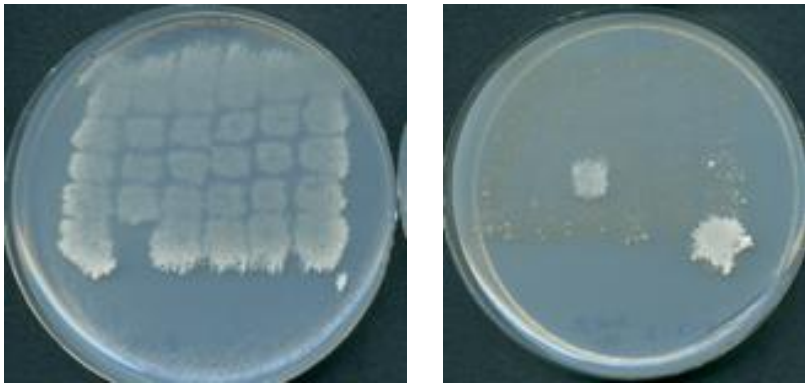

Figure 3. The T27P mutation creates a barrier for the transmission of the prion state from [*PIN*$^+$$_{WT}$] to Rnq1$_{T27P}$. (A) Scheme of experiment testing the frequency of [*PIN*$^+$] loss after substituting Rnq1$_{T27P}$ for Rnq1$_{WT}$. (B) Sample SD-Ade plates after [*PSI*$^+$] induction on SGal-SD-LeuHis. Shown is growth on SD-Ade after 14 days of incubation at 30^{0}C. All patches were Ade$^-$ after incubation on the control SD-LeuHis media (not shown). All patches were Ade$^-$ ([*pin*$^-$]) in the experiment where empty vector was substituted for Rnq1$_{WT}$ (not shown).

Figure 4

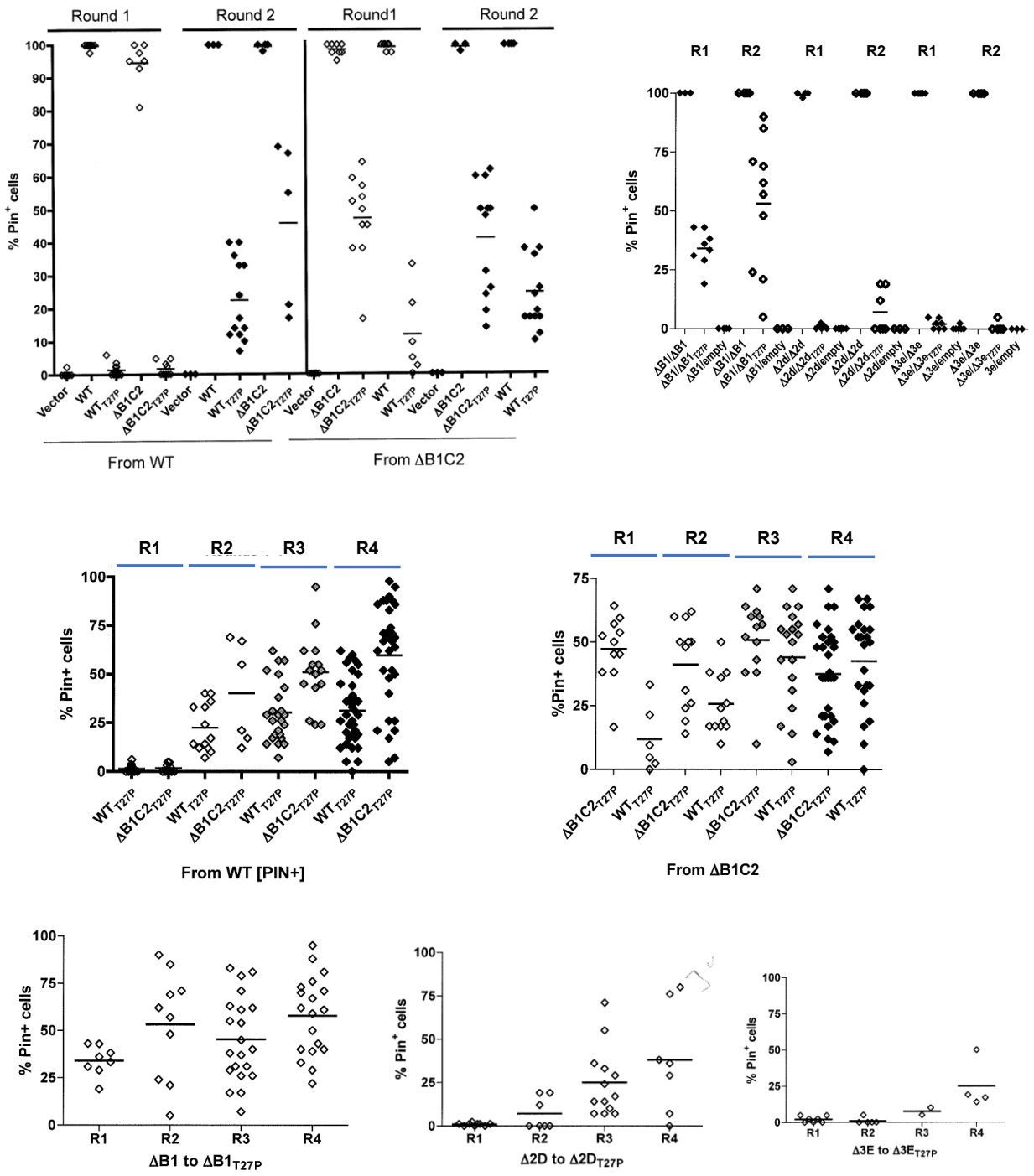

Figure 4. The transmission barrier created by the T27P mutation located in NPD is considerably reduced by the deletion of the first QN-rich region within Rnq1 PD. See text.

Figure 5

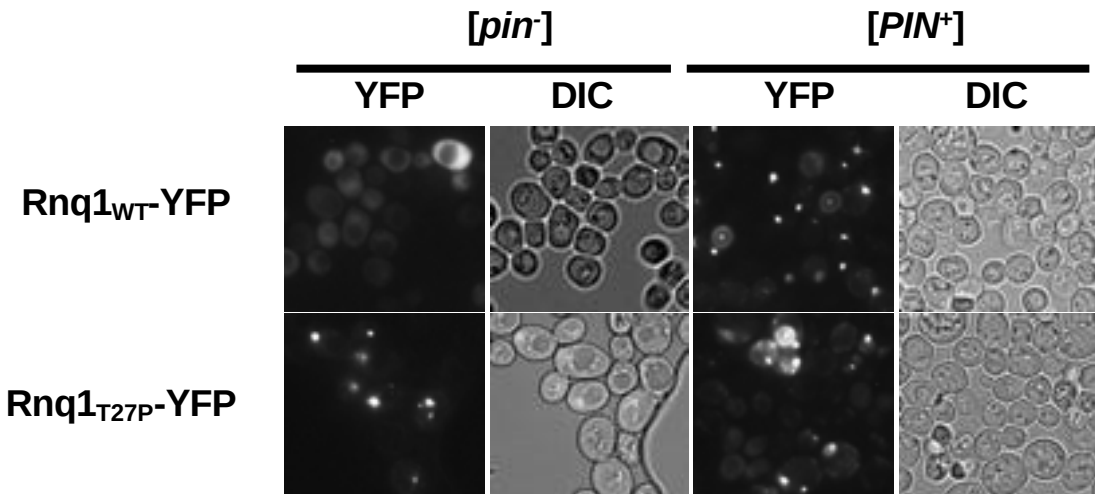

Figure 5. Dot-like aggregates are formed by Rnq1$_{T27P}$-YFP in [*pin*$^-$] cells. See text.